



An efficient computational method for global sensitivity analysis and its application to tree growth modelling

Qiong-Li Wu^{a,b,c,*}, Paul-Henry Cournède^{a,b}, Amélie Mathieu^d

^a INRIA Saclay Île-de-France, EPI DigiPlante, 91893 Orsay Cedex, France

^b Ecole Centrale de Paris, Laboratory MAS, 92290 Châtenay-Malabry Cedex, France

^c School of Electronic and Information Engineering, Wuhan University, Wuhan, China

^d UMR INRA/AgroParisTech Environnement et Grandes Cultures, 78850 Thiverval-Grignon, France

ARTICLE INFO

Article history:

Received 3 November 2010

Received in revised form

29 June 2011

Accepted 6 July 2011

Available online 19 July 2011

Keywords:

Sensitivity analysis

Sobol indices

Error estimation

Computing efficiency

Functional structural plant models

GreenLab

ABSTRACT

Global sensitivity analysis has a key role to play in the design and parameterisation of functional-structural plant growth models which combine the description of plant structural development (organogenesis and geometry) and functional growth (biomass accumulation and allocation). We are particularly interested in this study in Sobol's method which decomposes the variance of the output of interest into terms due to individual parameters but also to interactions between parameters. Such information is crucial for systems with potentially high levels of non-linearity and interactions between processes, like plant growth. However, the computation of Sobol's indices relies on Monte Carlo sampling and re-sampling, whose costs can be very high, especially when model evaluation is also expensive, as for tree models. In this paper, we thus propose a new method to compute Sobol's indices inspired by Homma–Saltelli, which improves slightly their use of model evaluations, and then derive for this generic type of computational methods an estimator of the error estimation of sensitivity indices with respect to the sampling size. It allows the detailed control of the balance between accuracy and computing time. Numerical tests on a simple non-linear model are convincing and the method is finally applied to a functional-structural model of tree growth, GreenLab, whose particularity is the strong level of interaction between plant functioning and organogenesis.

© 2011 Elsevier Ltd. All rights reserved.

1. Introduction

Sensitivity analysis (SA) is a fundamental tool in the building, use and understanding of mathematical models [1]. Sampling-based approaches to uncertainty and sensitivity analysis are both effective and widely used [2]. For this purpose, Sobol's method is a key one [3]. Since it is based on variance decomposition, the different types of sensitivity indices that it estimates can fulfill different objectives of sensitivity analysis: factor prioritisation, factor fixing, variance cutting or factor mapping [4]. It is a very informative method but potentially computationally expensive [2]. Besides the first-order effects, Sobol's method also aims at determining the levels of interaction between parameters [5]. In [6], the authors also devised a strategy for sensitivity analysis that could work for correlated input factors, based on the first-order and total-order index from variance decomposition.

Such type of global sensitivity analysis method has a key role to play in functional-structural plant growth modelling. In this recent field of research in plant biology [7] models are not yet stable. They aim at combining the description of both plant structural development and eco-physiological functioning at a very detailed scale, typically that of organs (leaves, internodes, etc.). The complexity of the underlying biological processes, especially the interaction between function and structure [8] usually makes parameterisation a complex step in modelling, and the analysis of model sensitivity to parameters and of their levels of interactions provides useful information in this process [9].

Computational methods to evaluate Sobol indices sensitivity rely on Monte Carlo sampling and re-sampling [3,10]. For k -dimensional factor of model uncertainty, the k first-order effects and the ' k ' total-order effects are rather expensive to estimate, needing a number of model evaluations strictly depending on k [11]. Especially, for individual-based tree growth models, at organ level, the cost of model evaluation can be very heavy [7]. Therefore, it is crucial to not only devise efficient computing techniques, in order to make best use of model evaluations [12], but also to have a good control of the estimation accuracy with respect to the number of samples.

* Corresponding author at: INRIA Saclay Île-de-France, EPI DigiPlante, 91893 Orsay Cedex, France.

E-mail address: qiongli.wu@gmail.com (Q.-L. Wu).

The objective of this paper is to study these two aspects. First, we propose a computing method inspired by [10], which improves slightly their use of model evaluations, and then derive an estimator of the error of sensitivity indices evaluation with respect to the sampling size for this generic type of computational methods. Numerical tests are then shown to illustrate the results. Finally, the method is applied to a functional–structural model of tree growth, whose particularity is the strong level of interaction between plant functioning and organogenesis [13].

2. Computing sensitivity analysis

2.1. General concepts of Sobol's sensitivity analysis

We recall here the basic concepts of Sobol's method [3] to present the original work about sensitivity analysis indices. The function $f(\mathbf{X}) \equiv f(X_1, X_2, \dots, X_k)$ under investigation is defined in the k -dimensional cube \mathbf{K}^k . If the input factors are mutually independent then there exists a unique decomposition of $f(\mathbf{X})$:

$$f(X_1, \dots, X_k) = f_0 + \sum_{i=1}^k f_i(X_i) + \sum_{1 \leq i < l \leq k} f_{il}(X_i, X_l) + \dots + f_{1,2,\dots,k}(X_1, \dots, X_k) \quad (1)$$

The basic idea of Sobol's method (see [3]) is to decompose the function of interest into terms of increasing dimensionality as in Eq. (1), such that all the summands are mutually orthogonal. The variance of the output variable Y can thus be decomposed into

$$V = \sum_{i=1}^k V_i + \sum_{1 \leq i < l \leq k} V_{il} + \dots + V_{1,2,\dots,k} \quad (2)$$

where V_i , V_{il} , $V_{1,2,\dots,k}$ denote the variance of f_i , f_{il} , $f_{1,2,\dots,k}$, respectively. In this approach the first-order sensitivity index for factor X_i is given by

$$S_i = \frac{V(E(Y|X_i))}{V(Y)} = \frac{V_i(E_{-i}(Y|X_i))}{V} \quad (3)$$

where E and V indicate, respectively, the mean and variance operators, $-i$ indicates all factors but i . The inner expectation is taken at a generic point in the space of variable X_i , while the outer variance is over all possible values of this generic point.

The higher order sensitivity indexes S_{i_1, \dots, i_s} are given by

$$S_{i_1, \dots, i_s} = \frac{V_{i_1, \dots, i_s}}{V} \quad (4)$$

for $s > 1$, Eq. (2) can be rewritten in terms of sensitivity indexes as

$$1 = \sum_{i=1}^k S_i + \sum_{1 \leq i < l \leq k} S_{il} + \dots + S_{1,2,\dots,k} \quad (5)$$

The total-order effect ST_i is instead given by

$$ST_i = \frac{E_{-i}(V_i(Y|X_{-i}))}{V} \quad (6)$$

Note that this time the inner variance is over all possible generic values of X_i while the outer mean is over the space X_{-i} . If $ST_i = 0$, then X_i is non-influent, so the index ST_i is suitable for fixing non-influential factors. Standard Sobol's method was proposed in [3]. In [10], an improved estimator is presented to compensate the system error, completed in [12], and a computationally efficient design is discussed. This method will therefore be called **Homma–Saltelli** method. We then propose an improvement of this method to promote its convergence characteristics.

2.2. Sobol's computing method and Homma–Saltelli (H–S) improvement

The standard Sobol's method for SA was put forward in [3], as one numerical simulation method to get the conditional expectation value for model output Y . We first decide the base sampling dimension N , then we implement the following steps:

1. Generate a Monte Carlo sampling of dimension N of the input factors according to their random distributions and form the $N \times k$ matrix $U_{N \times k}$ (k being the dimension of the input space) with each row a set of parameters; $U_{N \times k}$ is called the 'sampling matrix'

$$U_{N \times k} = \begin{bmatrix} X_{1(1)} & \dots & X_{i(1)} & \dots & X_{k(1)} \\ X_{1(2)} & \dots & X_{i(2)} & \dots & X_{k(2)} \\ \vdots & & \vdots & & \vdots \\ X_{1(N)} & \dots & X_{i(N)} & \dots & X_{k(N)} \end{bmatrix}$$

2. Generate another sampling matrix of dimension $N \times k$, $W_{N \times k}$, called the 're-sampling matrix'

$$W_{N \times k} = \begin{bmatrix} X_{1(N+1)} & \dots & X_{i(N+1)} & \dots & X_{k(N+1)} \\ X_{1(N+2)} & \dots & X_{i(N+2)} & \dots & X_{k(N+2)} \\ \vdots & & \vdots & & \vdots \\ X_{1(2N)} & \dots & X_{i(2N)} & \dots & X_{k(2N)} \end{bmatrix}$$

3. Define a matrix $W'_{N \times k}$ formed by all columns of $W_{N \times k}$, except the i th column obtained from the i th column of $U_{N \times k}$

$$W'_{N \times k} = \begin{bmatrix} X_{1(N+1)} & \dots & X_{i(1)} & \dots & X_{k(N+1)} \\ X_{1(N+2)} & \dots & X_{i(2)} & \dots & X_{k(N+2)} \\ \vdots & & \vdots & & \vdots \\ X_{1(2N)} & \dots & X_{i(N)} & \dots & X_{k(2N)} \end{bmatrix}$$

4. Compute the model output for each set of input parameters from $U_{N \times k}$ and $W'_{N \times k}$ (that is to say for each row in $U_{N \times k}$ and $W'_{N \times k}$) to obtain two column vectors of model outputs of dimension N : $\mathbf{y} = f(U_{N \times k})$, $\mathbf{y}'_R = f(W'_{N \times k})$.
5. The sensitivity indices are hence computed based on scalar products of the above-defined vectors of model outputs.

The applicability of the sensitivity estimates S_i to a large class of functions $f(\mathbf{X})$ is linked to the possibility of evaluating the multi-dimensional integral associated with these estimates via Monte Carlo methods. For a given sampling size N tending to ∞ the following estimate for the mean value of the output is straightforward:

$$\hat{f}_0 = \frac{1}{N} \sum_{j=1}^N \mathbf{y}^{(j)} \quad (7)$$

where $\mathbf{y}^{(j)}$ is the model output for a sample point in the parameter space \mathbf{K}^k . The hat symbol will be used to denote estimates.

To list the estimator for the standard Sobol's in [3], the following notation will be introduced:

$$\bar{V} = \frac{1}{N} \sum_{j=1}^N \mathbf{y}^{(j)2} \quad (8)$$

$$\bar{V}_i = \frac{1}{N} \sum_{j=1}^N \mathbf{y}^{(j)} \mathbf{y}_R^{(j)} \quad (9)$$

$$\bar{V}_{-i} = \frac{1}{N} \sum_{j=1}^N \mathbf{y}^{(j)} \mathbf{y}^{(j)} \quad (10)$$

Then we estimate the output variance by

$$\hat{V} = \bar{V} - \hat{f}_0^2 \quad (11)$$

$$V_i(E_{-i}(Y|X_i)) \approx \hat{V}_i = \bar{V}_i - \hat{f}_0^2 \quad (12)$$

$$V_{-i}(E_i(Y|X_{-i})) \approx \hat{V}_{-i} = \bar{V}_{-i} - \hat{f}_0^2 \quad (13)$$

and finally

$$\hat{S}_i = \frac{\hat{V}_i}{\hat{V}} = \frac{\bar{V}_i - \hat{f}_0^2}{\bar{V} - \hat{f}_0^2} \quad (14)$$

$$\hat{S}_{Ti} = 1 - \frac{\hat{V}_{-i}}{\hat{V}} = 1 - \frac{\bar{V}_{-i} - \hat{f}_0^2}{\bar{V} - \hat{f}_0^2} \quad (15)$$

As mentioned in [10], to compensate the ‘systematic error’ in standard Sobol’s method, better estimates for the term $V_i(E_{-i}(Y|X_i))$ is obtained by also computing the output of the ‘re-sampling matrix’ $W_{N \times k}$, we denote it as $\mathbf{y}_R = f(W_{N \times k})$. We define γ^2

$$\gamma^2 = \frac{1}{N} \sum_{j=1}^N \mathbf{y}^{(j)} \mathbf{y}_R^{(j)} \quad (16)$$

then the variance estimator is chosen as

$$V_i(E_{-i}(Y|X_i)) \approx \hat{V}_i = \bar{V}_i - \gamma^2 \quad (17)$$

For the same reason

$$\hat{S}_i = \frac{\hat{V}_i}{\hat{V}} = \frac{\bar{V}_i - \gamma^2}{\bar{V} - \gamma^2} \quad (18)$$

$$\hat{S}_{Ti} = 1 - \frac{\hat{V}_{-i}}{\hat{V}} = 1 - \frac{\bar{V}_{-i} - \gamma^2}{\bar{V} - \gamma^2} \quad (19)$$

In [12], a detailed proof of the cheaper computing cost for this method is given, and one conclusion is that by adding the computing cost of N model runs, we can get the full set of sensitivity indices (of all orders) for half the cost of the standard Sobol’s method [3]. For Homma–Saltelli method, to estimate each of the k first-order indices, the computing cost is $N(k+2)$ model runs, with N model runs for \mathbf{y} , N model runs for \mathbf{y}_R and Nk model runs for \mathbf{y}'_R . The same reasoning can be applied for ST_i , see Eq. (19). In the next section, we propose to adapt Homma–Saltelli method in order to slightly improve the use of model evaluations.

2.3. A new method to compute Sobol’s indices

The attempt for this improvement is to promote the computing efficiency and convergence of the method, and the basic idea is to make the sampling–re-sampling processing ‘smoother’ by ‘averaging’. In the Homma–Saltelli method, to compute $E_{-i}(Y|X_i)$, model outputs are computed for the $2N$ samplings of matrices ($U_{N \times k}$ and $W_{N \times k}$) and for the ‘re-sampling’ matrix ($W'_{N \times k}$). The complementary ‘re-sampling’ matrix $U'_{N \times k}$ can be defined and made full use of

$$U'_{N \times k} = \begin{bmatrix} \mathbf{x}_{1(1)} & \cdots & \mathbf{x}_{i(N+1)} & \cdots & \mathbf{x}_{k(1)} \\ \mathbf{x}_{1(2)} & \cdots & \mathbf{x}_{i(N+2)} & \cdots & \mathbf{x}_{k(2)} \\ \vdots & & & & \vdots \\ \mathbf{x}_{1(2N)} & \cdots & \mathbf{x}_{i(2N)} & \cdots & \mathbf{x}_{k(2N)} \end{bmatrix}$$

We denote $\mathbf{y}' = f(U'_{N \times k})$. Alternatively, \mathbf{y}' can also be used for $E_{-i}(Y|X_i)$. Correspondingly, when we average these two ways of computing $E_{-i}(Y|X_i)$, then the outer $V_i(E_{-i}(Y|X_i))$ should be inferior,

Table 1
Estimator improvement.

Variables	H-S	Proposed
\hat{f}_0	$\mathbf{y}^{(j)}$	$\frac{1}{2}(\mathbf{y}^{(j)} + \mathbf{y}_R^{(j)})$
\bar{V}_i	$\mathbf{y}^{(j)} \mathbf{y}_R^{(j)}$	$\frac{1}{2}(\mathbf{y}^{(j)} \mathbf{y}_R^{(j)} + \mathbf{y}_R^{(j)} \mathbf{y}^{(j)})$
\bar{V}_{-i}	$\mathbf{y}^{(j)} \mathbf{y}^{(j)}$	$\frac{1}{2}(\mathbf{y}^{(j)} \mathbf{y}^{(j)} + \mathbf{y}_R^{(j)} \mathbf{y}_R^{(j)})$
\bar{V}	$\mathbf{y}^{(j)^2}$	$\frac{1}{2}(\mathbf{y}^{(j)^2} + \mathbf{y}_R^{(j)^2})$
γ^2	$\mathbf{y}^{(j)} \mathbf{y}_R^{(j)}$	$\frac{1}{2}(\mathbf{y}^{(j)} \mathbf{y}_R^{(j)} + \mathbf{y}_R^{(j)} \mathbf{y}^{(j)})$

because by doing the averaging, we will get more ‘balanced’ simulation architecture. So we get the proposed variant Sobol’s estimator as shown in Table 1 according to the complementarity. The computing cost is mentioned as $N(k+2)$ for the old Sobol’s method to compute each of the k first-order indices [14]. For the estimator proposed in this paper, we make full use of the $2N$ samplings, just with Nk more model runs, that is to say with the computing cost of $N(2k+2)$ model runs. In order to fairly compare the efficiency of the two computing methods, we need to ensure the same number of model evaluations. It is thus obtained if the sampling size in the H-S method and new method obey $N_{H-S} = N_{new} * 2(k+1)/(k+2)$.

The test result will be given in Section 4. Before testing the estimator, we propose a way to evaluate the convergence characteristics of such type of computing methods.

3. Error estimation for Sobol’s method

3.1. Standard error, probable error

Assume function $f(\mathbf{X}) = f(x_1, x_2, \dots, x_k)$ under investigation is defined in the k -dimensional random variable space, the Monte Carlo method computing is applied to get the random distribution of $f(\mathbf{X})$ with N sampling points, then standard error is

$$\sigma(f) = \frac{1}{\sqrt{N}} \sqrt{\frac{1}{N} \sum_{n=1}^N f^2(\mathbf{X}_n) - \hat{f}_0^2} \quad (20)$$

with the distribution mean value

$$\hat{f}_0 = \frac{1}{N} \sum_{n=1}^N f(\mathbf{X}_n) \quad (21)$$

and its variance

$$\hat{V}(f) = \frac{1}{N} \sum_{n=1}^N f^2(\mathbf{X}_n) - \hat{f}_0^2 \quad (22)$$

In [10], the use of the probable error δ corresponding to the crude Monte Carlo method is computed like

$$\delta f = 0.6745 \times \sigma(f) \quad (23)$$

with the population f_0 having 50% chance of falling in the interval $f_0 \pm \delta f_0$. So, Eq. (20) is the form we adopt for the error estimate. Before we start for the probable error estimation of S_i ’s simulation result, we should make sure that Eq. (20) can be applied to our situation: first get the standard error of the considered variables, then we multiply the factor 0.6745 to get the probable error, based on the prerequisite that the variables should obey Gaussian distributions.

3.2. For Sobol’s formula

Error estimation is of crucial interest to check whether the SA computing has properly converged. Moreover, it can be used to give confidence bound of the result. Previous work as in [10] gave

interesting result about error estimation, but the conclusions are based on some restrictive assumptions:

- (1) It assumes that the problem under analysis is scaled before computing the variance, so that \hat{f}_0^2 is small.
- (2) The variance from \hat{f}_0^2 is neglected based on condition (1), so the variances of \hat{V} and \hat{V}_i are replaced by \bar{V} and \bar{V}_i . We thus perform a more comprehensive error estimation without considering these two hypotheses. We take the H-S Sobol's method for this error analysis. To get the error estimation for the new computing method proposed in Section 2.3, we simply need to replace the estimator in Table 1 with the improved ones, and change the denominator from N to $2N$.

3.2.1. Error estimation for S_i

Result 1. Approximation of the probable error for the computation of S_i is given by

$$\delta\hat{S}_i \approx 0.6745 \times \sigma\hat{S}_i = 0.6745 \times \sqrt{\frac{(\sigma\hat{V}_i)^2}{\hat{V}^2} + \frac{\hat{V}_i^2(\sigma\hat{V})^2}{\hat{V}^4} + 2\frac{\hat{V}_i(\sigma\hat{V})(\sigma\hat{V}_i)}{\hat{V}^3}} \quad (24)$$

Proof. Here we rewrite the formula for the Homma–Saltelli method to compute Sobol's indices:

$$\hat{S}_i = \frac{\hat{V}_i}{\hat{V}} = \frac{\bar{V}_i - \gamma^2}{\bar{V}} = \frac{\bar{V}_i - \gamma^2}{\bar{V} - \gamma^2} \quad (25)$$

We need to evaluate the standard error of the four items: $\sigma\bar{V}_i$, $\sigma\bar{V}$, $\sigma\gamma^2$ and $\sigma\hat{f}_0^2$. According to Eq. (20) for the definition of standard error and Eqs. (7), (9), (8), (16), for the computing of \hat{f}_0^2 , \bar{V}_i , \bar{V} , and γ^2 , respectively, then:

$$\sigma\bar{V}_i = \frac{1}{\sqrt{N}} \sqrt{\frac{1}{N} \sum_{j=1}^N [(\mathbf{y}^{(j)} \mathbf{y}_R^{(j)})^2] - \bar{V}_i^2} \quad (26)$$

$$\sigma\gamma^2 = \frac{1}{\sqrt{N}} \sqrt{\frac{1}{N} \sum_{j=1}^N [(\mathbf{y}^{(j)} \mathbf{y}_R^{(j)})^2] - ((\gamma^2)^2)} \quad (27)$$

$$\sigma\bar{V} = \frac{1}{\sqrt{N}} \sqrt{\frac{1}{N} \sum_{j=1}^N [(\mathbf{y}^{(j)})^2] - \bar{V}^2} \quad (28)$$

$$\sigma\hat{f}_0^2 = \frac{1}{\sqrt{N}} \sqrt{\frac{1}{N} \sum_{j=1}^N [(\mathbf{y}^{(j)})^2] - \hat{f}_0^2} \quad (29)$$

According to Eq. (A.6) in Appendix, the variance for \hat{f}_0^2 is

$$V_{\hat{f}_0^2} = (\sigma\hat{f}_0^2)^2 = (2 \times \hat{f}_0 \times \sigma\hat{f}_0)^2 \quad (30)$$

So

$$\sigma\hat{f}_0^2 = (2 \times \hat{f}_0 \times \sigma\hat{f}_0) \quad (31)$$

and using Eq. (A.8) giving the variance of a sum of random variables:

$$\sigma\hat{V} = \sqrt{V_{\bar{V}} + V_{\hat{f}_0^2} - 2 \text{cov}(\bar{V}, \hat{f}_0^2)} \quad (32)$$

Since \bar{V} and \hat{f}_0^2 use the same set of samples, the correlation index ρ can be approximated to be 1 here, so

$$\text{cov}(\bar{V}, \hat{f}_0^2) = \rho \sqrt{V_{\bar{V}}} \sqrt{V_{\hat{f}_0^2}} \approx \sqrt{V_{\bar{V}}} \sqrt{V_{\hat{f}_0^2}} = \sigma\bar{V} \sigma\hat{f}_0^2 \quad (33)$$

Then

$$\sigma\hat{V} \approx \sqrt{(\sigma\bar{V})^2 + (\sigma\hat{f}_0^2)^2 - 2\sigma\bar{V}\sigma\hat{f}_0^2} \approx |\sigma\bar{V} - \sigma\hat{f}_0^2|$$

so

$$\sigma\hat{V} \approx |\sigma\bar{V} - \sigma\hat{f}_0^2| \approx \left| \sqrt{\frac{1}{N} \left(\sum_{j=1}^N [(\mathbf{y}^{(j)})^2] - \bar{V}^2 \right)} - 2 \times \hat{f}_0 \times \sigma\hat{f}_0 \right|$$

Likewise, for $\sigma\hat{S}_i$ with $\hat{V}_i = \bar{V}_i - \gamma^2$, and correlation coefficient of \bar{V}_i and γ^2 set to 1:

$$\sigma\hat{V}_i \approx |\sigma\bar{V}_i - \sigma\gamma^2| \quad (34)$$

We then use Eq. (A.10) given in Appendix to estimate the variables of \hat{V}_i/\bar{V} , but we have the same problem to get the correlation index of \hat{V}_i and \bar{V} , and it is not 1 anymore, because they do not share the same sample. However, to make sure that we will get the 'upper bound' of the real variance, we consider the least favorable case, obtained for a correlation of -1 , that is to say: $\text{cov}(\bar{V}_i, \bar{V}) \approx -\sigma\bar{V}\sigma\bar{V}_i$ and then

$$\sigma\hat{S}_i = \sqrt{\frac{(\sigma\hat{V}_i)^2}{\hat{V}^2} + \frac{\hat{V}_i^2(\sigma\hat{V})^2}{\hat{V}^4} + 2\frac{\hat{V}_i(\sigma\hat{V})(\sigma\hat{V}_i)}{\hat{V}^3}} \quad (35)$$

according to Eq. (23) about the relationship between probable error and standard error, So

$$\begin{aligned} \delta\hat{S}_i &\approx 0.6745 \times \sigma\hat{S}_i \\ &= 0.6745 \times \sqrt{\frac{(\sigma\hat{V}_i)^2}{\hat{V}^2} + \frac{\hat{V}_i^2(\sigma\hat{V})^2}{\hat{V}^4} + 2\frac{\hat{V}_i(\sigma\hat{V})(\sigma\hat{V}_i)}{\hat{V}^3}} \quad \square \end{aligned} \quad (36)$$

3.2.2. Error estimation for ST_i

Result 2. Approximation of the probable error for the computation of ST_i is given by

$$\begin{aligned} \delta\hat{ST}_i &\approx 0.6745 \times \sigma\hat{ST}_i \\ &= 0.6745 \times \sqrt{\frac{(\sigma\hat{V}_{-i})^2}{\hat{V}^2} + \frac{\hat{V}_{-i}^2(\sigma\hat{V})^2}{\hat{V}^4} + 2\frac{\hat{V}_{-i}(\sigma\hat{V})(\sigma\hat{V}_{-i})}{\hat{V}^3}} \end{aligned} \quad (37)$$

Proof. As we check Eq. (19), we can get that the error estimation for ST_i is similar as for S_i , the difference is changing $\sigma\hat{V}_i$ to $\sigma\hat{V}_{-i}$ and changing \bar{V}_i to \bar{V}_{-i} in Eq. (24), and we can easily get that

$$\sigma\bar{V}_{-i} = \frac{1}{\sqrt{N}} \sqrt{\frac{1}{N} \sum_{j=1}^N [(\mathbf{y}^{(j)} \mathbf{y}'^{(j)})^2] - \bar{V}_{-i}^2} \quad (38)$$

so as in Eq. (34)

$$\sigma\hat{V}_{-i} = |\sigma\bar{V}_{-i} - \sigma\gamma^2| \quad (39)$$

finally

$$\begin{aligned} \delta\hat{ST}_i &\approx 0.6745 \times \sigma\hat{ST}_i \\ &= 0.6745 \times \sqrt{\frac{(\sigma\hat{V}_{-i})^2}{\hat{V}^2} + \frac{\hat{V}_{-i}^2(\sigma\hat{V})^2}{\hat{V}^4} + 2\frac{\hat{V}_{-i}(\sigma\hat{V})(\sigma\hat{V}_{-i})}{\hat{V}^3}} \quad \square \end{aligned} \quad (40)$$

4. Computational tests

4.1. Analytical functions

To demonstrate the performance of the error estimation and the efficiency of the proposed method, an artificial analytical

model with three input variables (Ishigami Function) is considered, as in [15]:

$$f(X_1, X_2, X_3) = \sin X_1 + a \sin^2 X_2 + b X_3^4 \sin X_1 \quad (41)$$

where its input probability density functions (pdf) is as follows:

$$p_i(X_i) = \begin{cases} \frac{1}{2\pi}, & -\pi \leq X_i \leq \pi, \\ 0, & X_i < -\pi \text{ or } X_i > \pi, \end{cases} \quad i = 1, 2, 3$$

from Eq. (2), the total variance V and partial variances V_i can be obtained analytically as

$$V = \frac{a^2}{8} + \frac{b\pi^4}{5} + \frac{b^2\pi^8}{18} + \frac{1}{2} \quad (42)$$

$$V_1 = \frac{b\pi^4}{5} + \frac{b^2\pi^8}{50} + \frac{1}{2} \quad (43)$$

$$V_2 = \frac{a^2}{8} \quad (44)$$

$$V_3 = 0 \quad (45)$$

In our test case, the constants in Eqs. (42)–(45) are given the values $a=7$ and $b=0.1$. We use the ‘Mersenne Twister random number generator’ to get the random sampling for the three input parameters.

4.2. Error estimation test

The purpose of this test is to examine how the error estimation works in the Monte Carlo computation of sensitivity with the comparison between the ones computed analytically from Eqs. (24) and (37), respectively, for $\delta\hat{S}_i$, $\delta\widehat{ST}_i$ and those obtained by

repeating the computation of SA indices for a number of times (with different seeds for the MT generator) are denoted by $\delta\hat{S}_i^*$, $\delta\widehat{ST}_i^*$. NbR will denote the number of repetitions. All the data shown here are calculated using combined data from all runs. We use the Homma–Saltelli Sobol’s estimator in this test case in order to compare the error estimation with those obtained in the previous works in [10], denoted by $\delta\widehat{S}_{i_{ref}}$, $\delta\widehat{ST}_{i_{ref}}$.

Since the set of all S_i plus the set of all ST_i give a fairly good description of the model sensitivities, here we only give these two sets of indices for the test.

As shown in Tables 2 and 3, we can see that the theoretical upper bound error estimation $\delta\hat{S}_i$, $\delta\widehat{ST}_i$ is very effective compared to the one we computed by numerical simulations $\delta\hat{S}_i^*$, $\delta\widehat{ST}_i^*$, while it is much more accurate than the previous work $\delta\widehat{S}_{i_{ref}}$, $\delta\widehat{ST}_{i_{ref}}$. So the proposed error estimation can be a good indication to judge the level of accuracy of the SA index computation, according to which we can find a proper number of sampling (NbS) for SA.

4.3. Comparison of H–S and proposed method

We compare the Homma–Saltelli (H–S) method and the proposed new one in Tables 4 and 5, with the same model evaluation computing cost corresponding to different numbers of samplings as explained in Section 2.3. As we mentioned in Section 2.3, $N_{H-S} = N_{new} * 2(k+1)/(k+2)$, here $k=3$ for our test case, when $N_{new} = 1000$, then $N_{H-S} = 1600$. We can see that, both for S_i and ST_i , our proposed new method can provide more stable results, that is to say, it can get the result with less variance, as also confirmed by our standard error estimation. This result agrees with our expectation that the complimentary characteristic of the sampling matrix and re-sampling matrix can help to

Table 2

H–S Sobol’s method for S_i , same number of runs (NbR=100), different numbers of samplings (NbS).

Variables	$S_i(\text{exact})$	\hat{S}_i	Bias	$\delta\hat{S}_i$	$\delta\widehat{S}_{i_{ref}}$	$\delta\hat{S}_i^*$
NbS=10						
X_1	0.3138	0.332128893	0.018328893	0.420126891	0.64922391	0.394116208
X_2	0.4424	0.576970598	0.134570598	0.441915034	0.799264515	0.459467686
X_3	0	−0.047977424	0.047977424	0.368651048	0.40482392	0.329106545
NbS=100						
X_1	0.3138	0.317898441	0.00409844	0.113155712	0.17496605	0.098588362
X_2	0.4424	0.44332627	0.00092627	0.110788108	0.19688452	0.072259899
X_3	0	0.014475517	0.014475517	0.126772756	0.129683521	0.082991208
NbS=1000						
X_1	0.3138	0.31704138	0.00324138	0.035478791	0.056020475	0.029357167
X_2	0.4424	0.44426211	0.00186211	0.034121285	0.062915907	0.029415413
X_3	0	0.003420994	0.003420994	0.040333006	0.040555193	0.02417304

Table 3

H–S Sobol’s method for ST_i , same number of runs (NbR=100), different numbers of samplings (NbS).

Variables	$ST_i(\text{exact})$	\widehat{ST}_i	Bias	$\delta\widehat{ST}_i$	$\delta\widehat{ST}_{i_{ref}}$	$\delta\widehat{ST}_i^*$
NbS=10						
X_1	0.5574	0.471006778	0.086393222	0.587139075	0.773255643	0.452078804
X_2	0.4442	0.433857546	0.010342454	0.470375601	0.80001505	0.419140296
X_3	0.241	0.09090012	0.15009988	0.518931875	1.04536509	0.45891867
NbS=100						
X_1	0.5574	0.54219821	0.01520179	0.123465946	0.21247326	0.11183428
X_2	0.4442	0.457708634	0.013508634	0.126828544	0.23284288	0.08433098
X_3	0.241	0.238775324	0.002224676	0.1248745	0.26201749	0.114110644
NbS=1000						
X_1	0.5574	0.55231685	0.00508315	0.038581076	0.067597875	0.037170484
X_2	0.4442	0.43980209	0.00439791	0.040345109	0.076681373	0.028618586
X_3	0.241	0.23869646	0.00230354	0.035262641	0.084598942	0.034681808

Table 4
Efficiency comparison of H–S and our new Sobol's method for S_i , with the same number of model evaluations, H–S method with number of samplings (NbS=1600), number of runs (NbR=100), new method with number of samplings (NbS=1000), number of runs (NbR=100).

Variables	$S_i(\text{exact})$	\hat{S}_i	Bias	$\delta\hat{S}_i$	$\delta\hat{S}_{i_{ref}}$	$\delta\hat{S}_i^*$
<i>H–S</i>						
X_1	0.3138	0.31533298	0.00153298	0.02799958	0.044172429	0.022979037
X_2	0.4424	0.44665802	0.00425802	0.027065163	0.049959473	0.020148217
X_3	0	−0.000991375	0.000991375	0.031977602	0.031926896	0.018688355
<i>New</i>						
X_1	0.3138	0.31298693	0.00081307	0.024947723	0.051779454	0.014254
X_2	0.4424	0.44600325	0.00360325	0.024195279	0.062443818	0.014995118
X_3	0	−0.000171562	0.000171562	0.028633187	0.02861765	0.01049768

Table 5
Efficiency comparison of H–S and our new Sobol's method for ST_i , with the same number of model evaluations, H–S method with number of samplings (NbS=1600), number of runs (NbR=100), new method with number of samplings (NbS=1000), number of runs (NbR=100).

Variables	$ST_i(\text{exact})$	\hat{ST}_i	Bias	$\delta\hat{ST}_i$	$\delta\hat{ST}_{i_{ref}}$	$\delta\hat{ST}_i^*$
<i>H–S</i>						
X_1	0.5574	0.55433338	0.00306662	0.030524063	0.053367661	0.028061632
X_2	0.4442	0.44145391	0.00274609	0.031846525	0.060492716	0.024130443
X_3	0.241	0.24447647	0.00347647	0.027831009	0.066898161	0.02334635
<i>New</i>						
X_1	0.5574	0.55543245	0.00196755	0.027455945	0.065578754	0.018760671
X_2	0.4442	0.44419771	2.29E-06	0.028548756	0.076191397	0.01669605
X_3	0.241	0.23800909	0.00299091	0.024822554	0.089599272	0.022789275

get a more ‘balanced’ result. Other types of estimators for Sobol indices exist in the literature. In a recent paper [11], the authors compared different types of estimators for ST_i , and ‘Jansen’s’ [16] estimator is shown to be the most efficient. It would thus be interesting to adapt the strategy proposed in this paper to other estimators to check whether the same convergence characteristics can be obtained.

5. Model application: GreenLab tree growth model

5.1. Description of the case study

GreenLab is a functional–structural plant model that simulates plant development, growth and morphology [17]. The plant growth is discretized with a time step corresponding to the architectural growth cycle, that is to say the time necessary to set in place new growth units (e.g., 1 year for tree in temperate climate). Regarding plant architecture, trees are decomposed into elementary units called phytomers that are gathered into categories according to morphological properties [18]. These categories are indexed by a variable called physiological age, from 1 for the trunk to P_m for the small twigs. P_m is taken as 4 in our test case, which is generally sufficient to describe complex trees. A time step starts with the appearance of the new organs on the plant, and the tree architecture remains constant during the whole time step.

Interactions between plant organogenesis and functional mechanisms have been implemented by linking the number of new organs to the ratio of available biomass to plant demand. The main equations of the model are given in the following of the section but a complete description can be read in [13]. Note however that we restrict the study to a theoretical tree (with strong similarities in terms of behaviour with the poplar tree) and simplify the ecophysiological sub-models for the sake of clarity.

For the sensitivity analysis, the variable of interest is the amount of biomass produced at each time step denoted by n .

For this study, it is computed with a simple empirical equation adapted from the Beer–Lambert law:

$$Q(n) = E_{PAR}(n)\mu S_p(1 - \exp^{-\kappa(S_f(n)/S_p)}) \tag{46}$$

$E_{PAR}(n)$ denotes the amount of photosynthetically active radiation received by the plant during the whole time step n , $\mu = 0.33$ is an efficiency simulating the conversion of light energy into biomass, S_p is an empirical coefficient linked to the projected ground surface, κ denotes the extinction coefficient of the Beer–Lambert law. $S_f(n)$ is the whole leaf surface area of the tree. It is the sum of each individual leaf surface area. Leaves are assumed to have a constant leaf mass per area $e = 0.03 \text{ g cm}^{-2}$, allowing to deduce their surfaces from their masses.

The amount of biomass $Q(n)$ will be used for secondary growth and growth of new organs at the next time step. The allocation model is a proportional one, which means that the biomass allocated to an organ is proportional to its sink strength divided by the plant demand, that is the sum of the organ sink strengths. The biomass used for the secondary growth is proportional to the number of leaves, in accordance with the pipe model theory [19]. The number of functional buds, i.e., the ones that will give birth to a branch, and the number of phytomers on each branch depends on the ratio of available biomass to demand, see [13] for detailed equations. This key variable is correlated to the amount of biomass allocated to new organs denoted by $Q_B(n)$. Finally, the tree leaf surface area is given by the equation:

$$S_f(n) = \frac{1}{e} \sum_{k=1}^{P_m} p_B^k \frac{S_B^k Q_B(n)}{d_B^k \cdot D_{fb}(n)} \tag{47}$$

p_B^k and S_B^k denote, respectively, the sink strength of buds and leaves of physiological age k , d_B^k denote the demand of the corresponding growth unit and $D_{fb}(n)$ is the demand of these buds. For this case study, $S_B=1$, $S_f=1$ and $S_L=0.1$ denote, respectively, the sink strengths for blades, internodes and layers. They have the same values for each physiological age.

The plant behaviour is the result of the interactions between organogenesis and photosynthesis. When there is enough available biomass, the ratio of biomass to demand is high and a lot of leaves will appear in the tree. As the demand is proportional to the number of leaves, the increase in the number of leaves induces an increase in plant demand and consequently a decrease in the ratio of biomass to demand. The number of new leaves will decrease, inducing a low demand and a high ratio of biomass to demand, and so on. For some combination of the parameters, rhythms may appear in plant biomass production and topology [20]. We choose such a case study for this article, as illustrated by the trend of the ratio of available biomass to demand (Fig. 1). Fig. 2 shows the plant structure after 30 years.

5.2. Sensitivity analysis for the tree growth model

The sensitivity analysis method was applied to the tree annual biomass production computed with Eq. (46). As mentioned in [9], linearity index is first checked before starting global SA. At the beginning of plant growth, the model is close to linear (Fig. 3). Then for some growth stages, the linearity index decreases to reach a value lower than 0.5. At this stage, the biomass production is low, because of a small number of leaves (Fig. 4) induced by a lower ratio of biomass to demand (Fig. 1). The sensitivity index of the model for parameter R follows the pattern of biomass production (Fig. 5).

Due to the exponential negative function, the biomass production is very sensitive in changes in total leaf surface area when this one is small, but on the contrary, there is a value beyond which an increase in leaf surface area will induce a very little increase in biomass production. As the leaf surface area depends on the number of organs, the biomass production alternates between the phase close to saturation and the linear phase. In the linear phase, the model is more sensitive to the parameter S_p . On the contrary, in the saturation phase, the model is more sensitive to the parameter μ as illustrated by Fig. 5.

These two parameters are the most important ones regarding biomass production. We exclude these two parameters to get closer inspect for the other parameters driving biomass allocation – sink strengths – that impact plant production through the

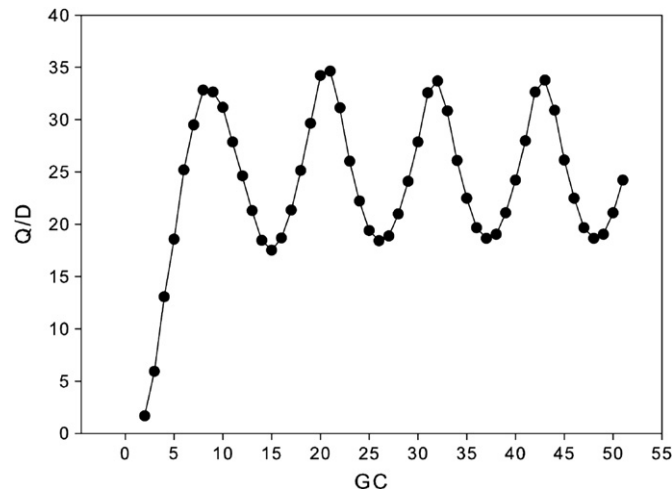


Fig. 1. Oscillations in the ratio of available biomass to demand for the modelled tree. First the ratio increases due to an increase in biomass production at a constant level of demand. When its value exceeds a threshold, new organs appear, which leads to an increase in plant demand and hence a decrease of the ratio. The ratio falls below the threshold, allowing a smaller number of leaves to emerge, and a decrease in the demand and so on.

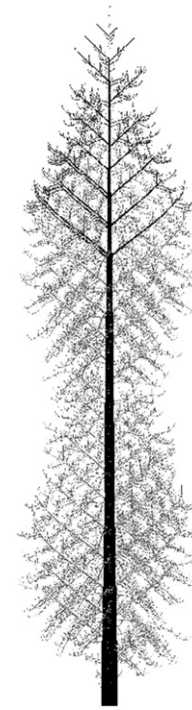


Fig. 2. Plant topology after 30 time steps. The light grey branches are the dead ones. The living branches of different physiological ages are represented by different levels of grey to illustrate the morphogenetic gradient in tree architecture, starting with Physiological Age 1 in black.

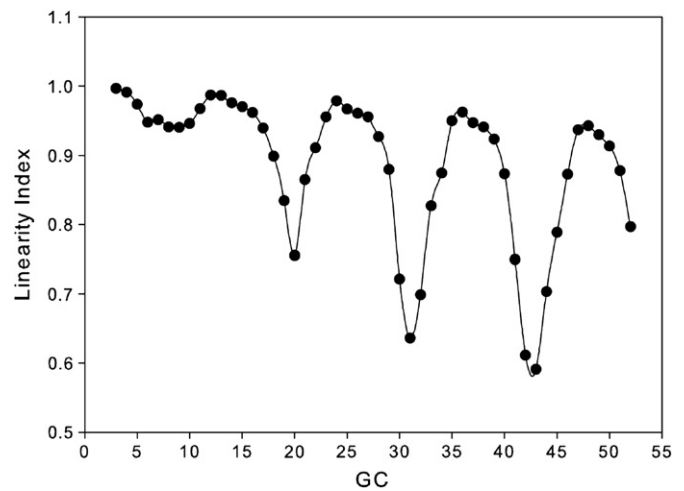


Fig. 3. Linearity index of the model.

computation of leaf surface area (Eq. (47)), as shown in Fig. 6. In the youth of the tree, the trunk starts growing and no branch appear due to the low value of the ratio of biomass to demand. At this point, the model is mainly sensitive to the parameters of phytomers of physiological age 1 ($(S_B)_0$ and $(S_I)_0$ in Fig. 6). Then, the ratio of available biomass to demand increases fast, and several branches appear together. The phytomers of physiological age 4 are the more numerous in the tree as they correspond to the twigs. Their number increases till the time step 15 and then oscillates (Fig. 4), with a period corresponding to the ratio of biomass to demand (Fig. 1). Hence, the model output is sensitive to their sink strengths ($(S_B)_3$, $(S_I)_3$ and $(S_I)_3$ in Fig. 6) with the same period.

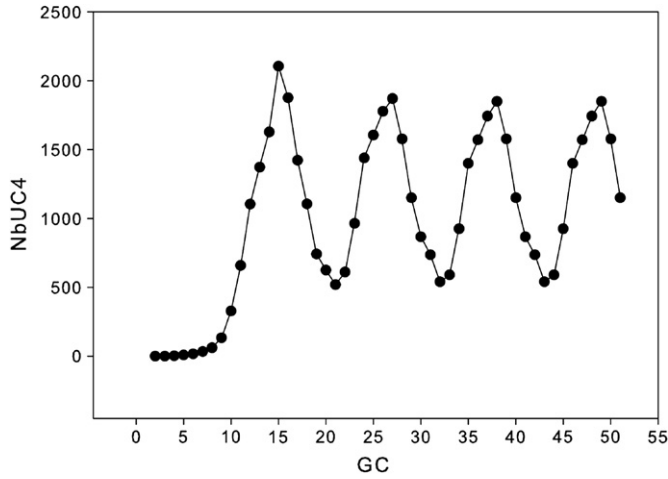


Fig. 4. Number of phytomers of physiological age 4. Their number depends on the ratio of available biomass to demand.

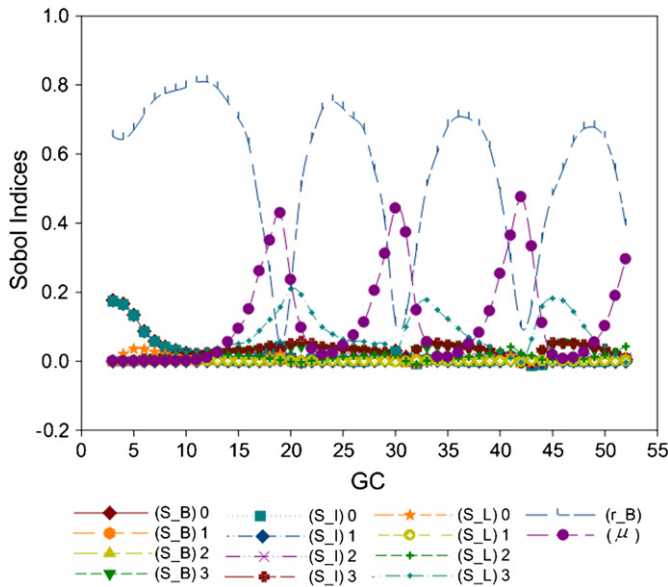


Fig. 5. Sensitivity indexes for all the model parameters.

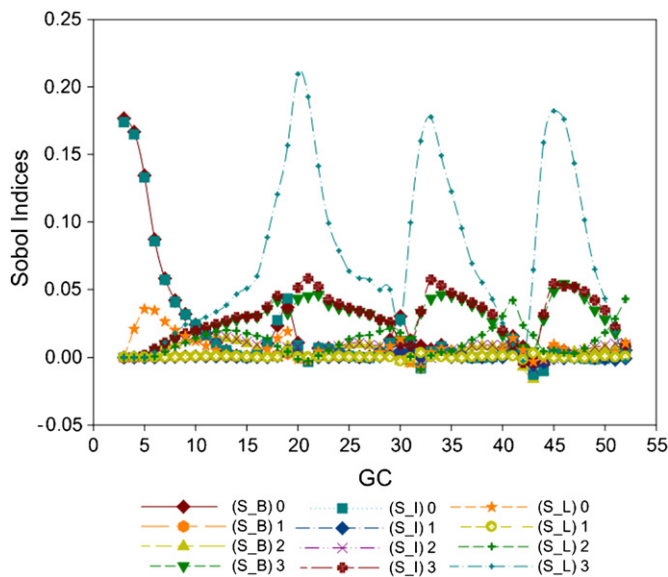


Fig. 6. Sensitivity indices when fixing μ and S_p .

6. Discussion

With the objective of an efficient computational method for sensitivity analysis of functional–structural tree growth models, we proposed a new estimator based on the Homma–Saltelli method to compute Sobol's indices. This new estimator can be considered as an effort to improve the efficiency of SA methods for models.

Another problem brought by this sampling-based computing strategy is to get results as accurate as possible but with as few samples as possible. We generally lack benchmarks to control the convergence of computing methods. Most of the time we do not have the analytical result for the sensitivity indices. Therefore, we derived a theoretical analysis of the error estimation for the sensitivity analysis for the class of Sobol's estimators (it can be applied to all the three Sobol's estimators mentioned in this paper). An analytical test function is used to test the error estimation, and we obtained that the error estimation in this paper gives out a better 'upper bound' than the previous works related to this problem. This error estimation directly relates to the variance of the result, so it can also be used for checking the confidence interval, which is usually difficult to attain.

The computation method for Sobol indices as well as the error estimation can also be performed with other types of random number generator which are proved to also have an important influence on the efficiency of the algorithms [11], therefore, same tests were performed with quasi-random generator [11] leading to the same conclusions. As an application, we applied the new method to a tree growth model characterized by a strong level of interactions. We inspected 14 parameters related to tree biomass production and allocation, and follow dynamically the sensitivity indices for 50 years. Note that the computation of such a long period of growth remains quite reasonable for the GreenLab model thanks to the structural factorisation described in [17]. The test case chosen corresponds to a specific model showing alternating patterns in growth phases resulting from the complex interactions between functioning and organogenesis. The sensitivity analysis offered interesting insight in the understanding of this interaction. Moreover, by using variance-based techniques, an analyst is capable not only of obtaining the parameter contribution to the output variance but also of gaining insights on the model structure by using moment-independent indicators [21]. Such method provides insights on the influence of the input uncertainty on the output distribution [22]. So it would be interesting for our future work to gain insight about the output distribution (in our tree modelling case, for the variables describing tree height and diameter for example). It should open a new way to deeper studies on more complex functional–structural plant models.

Appendix A. Taylor expansions to approximate the moments of functions of random variables

It is possible to approximate the moments of a function f of random variables X, Y using Taylor expansions, provided that f is sufficiently differentiable and that the moments of X and Y are finite [23]. Let us denote the expectations $E(X) = \mu_X$, $E(Y) = \mu_Y$, and variances $V(X) = \sigma_X^2$, $V(Y) = \sigma_Y^2$. We thus get the following results:

- Suppose $Z = f(X)$, then

$$E(Z) \approx f(\mu_X) + \frac{f''(\mu_X)}{2} \sigma_X^2 \quad (\text{A.1})$$

$$V(Z) \approx [f'(\mu_X) \sigma_X]^2 \quad (\text{A.2})$$

- Suppose $Z = f(X, Y)$, then

$$E(Z) \approx f(\mu_X, \mu_Y) + \frac{1}{2} f_{xx}(\mu_X, \mu_Y) \sigma_X^2 + f_{xy}(\mu_X, \mu_Y) \text{cov}(X, Y) + \frac{1}{2} f_{yy}(\mu_X, \mu_Y) \sigma_Y^2 \quad (\text{A.3})$$

$$V(Z) \approx [f_x(\mu_X, \mu_Y) \sigma_X]^2 + [f_y(\mu_X, \mu_Y) \sigma_Y]^2 + 2 f_{xy}(\mu_X, \mu_Y) f_y(\mu_X, \mu_Y) \text{cov}(X, Y) \quad (\text{A.4})$$

In particular,

- if $Z = X^2$, then

$$E[Z] = \mu_X^2 + \sigma_X^2 \quad (\text{A.5})$$

$$V[Z] \approx 4\mu_X^2 \sigma_X^2 \quad (\text{A.6})$$

- and if $Z = X \pm Y$, then

$$E[Z] = \mu_X \pm \mu_Y \quad (\text{A.7})$$

$$V[Z] = \sigma_X^2 + \sigma_Y^2 \pm 2 \text{cov}(X, Y) \quad (\text{A.8})$$

- and if $Z = X/Y$, then

$$E[Z] \approx \frac{\mu_X}{\mu_Y} - \frac{1}{\mu_Y^2} \text{cov}(X, Y) + \frac{\mu_X \cdot \mu_Y}{\mu_Y^4} \cdot \sigma_Y^2 \quad (\text{A.9})$$

$$V[Z] \approx \frac{1}{\mu_Y^2} \cdot \sigma_X^2 - 2 \cdot \frac{\mu_X}{\mu_Y^3} \cdot \text{cov}(X, Y) + \frac{\mu_X^2}{\mu_Y^4} \cdot \sigma_Y^2 \quad (\text{A.10})$$

References

- [1] Saltelli A, Ratto M, Andres T, Campolongo F, Cariboni J, Gatelli D, et al. Global sensitivity analysis. the primer ed.. John Wiley & Sons; 2008.
- [2] Helton J, Johnson J, Salaberry C, Storlie C. Survey of sampling based methods for uncertainty and sensitivity analysis. Reliability Engineering and System Safety 2006;91:1175–209.
- [3] Sobol I. Sensitivity analysis for non-linear mathematical models. Mathematical Modeling and Computational Experiment 1993;1:407–14.
- [4] Cariboni J, Gatelli D, Liska R, Saltelli A. The role of sensitivity analysis in ecological modelling. Ecological modelling 2007;203:167–82.
- [5] Wu QL, Cournède PH. The use of sensitivity analysis for the design of functional structural plant models. In: Procedia—Social and behavioral sciences, sixth international conference on sensitivity analysis of model output, vol. 2, issue 6; 2010. p. 7768. doi:10.1016/j.sbspro.2010.05.219.
- [6] Saltelli A, Tarantola S. On the relative importance of input factors in mathematical models: safety assessment for nuclear waste disposal. Journal of American Statistical Association 2002;97:702–9.
- [7] Sievanen R, Nikinmaa E, Nygren P, Ozier-Lafontaine H, Perttunen J, Hakula H. Components of a functional–structural tree model. Annals of Forest Sciences 2000;57:399–412.
- [8] Vos J, Evers J, Buck-Sorlin G, Andrieu B, Chelle M, de Visser P. Functional–structural plant modelling: a new versatile tool in crop science. Journal of Experimental Botany 2009.
- [9] Wu QL, Cournède PH. Sensitivity analysis of greenlab model for maize. In: Li B, Jaeger M, Guo Y, editors. Third international symposium on plant growth and applications (PMA 09). Beijing, China (PMA 09): IEEE; 2009.
- [10] Homma T, Saltelli A. Importance measures in global sensitivity analysis of nonlinear models. Reliability Engineering and System Safety 1996;52:1–17.
- [11] Saltelli A, Annoni P, Azzini I, Campolongo F, Ratto M, Tarantola S. Variance based sensitivity analysis of model output, design and estimator for the total sensitivity index. Computer Physics Communications 2010;181(2):259–70.
- [12] Saltelli A. Making best use of model evaluations to compute sensitivity indices. Computer Physics Communications 2002;145:280–97.
- [13] Mathieu A, Cournède P, Letort V, Barthélémy D, de Reffye P. A dynamic model of plant growth with interactions between development and functional mechanisms to study plant structural plasticity related to trophic competition. Annals of Botany 2009;103:1173–86.
- [14] Pagano A, Ratto M. An extended use of the sobol' estimator. In: The fifth international conference on sensitivity analysis of model output—SAMO 2007.
- [15] Ishigami T, Homma T. An importance quantification technique in uncertainty analysis for computer models. In: Proceedings of the ISUMA'90, first international symposium on uncertainty modelling and analysis. USA: University of Maryland; 1990. p. 398–403.
- [16] Jansen MJ. Analysis of variance designs for model output. Computer Physics Communications 1999;117(1–2):35–43.
- [17] Cournède PH, Kang MZ, Mathieu A, Barczi JF, Yan HP, Hu BG, et al. Structural factorization of plants to compute their functional and architectural growth. Simulation 2006;82(7):427–38.
- [18] Barthélémy D, Caraglio Y. Plant architecture: a dynamic, multilevel and comprehensive approach of plant form, structure and ontogeny. Annals of Botany 2007;99:375–407.
- [19] Shinozaki K, Yoda K, Hozumi K, Kira T. A quantitative analysis of plant form—the pipe model theory. I. Basic analysis. Japanese Journal of Ecology 1964;14:97–105.
- [20] Mathieu A, Cournède P, Barthélémy D, de Reffye P. Rhythms and alternating patterns in plants as emergent properties of a model of interaction between development and functioning. Annals of Botany 2008;101(8):1233–42.
- [21] Borgonovo E. Measuring uncertainty importance: investigation and comparison of alternative approaches. Risk Analysis 2006;26:1349–61.
- [22] Borgonovo E. A new uncertainty importance measure. Reliability Engineering & System Safety 2007;92(6):771–84.
- [23] Bevington PR, Robinson DK. Data reduction and error analysis for the physical sciences. Boston, MA: McGraw-Hill; 2003.